

Molecular dynamics simulations of ramp-compressed copperA. Higginbotham,¹ J. Hawreliak,² E. M. Bringa,³ G. Kimminau,¹ N. Park,⁴ E. Reed,² B. A. Remington,² and J. S. Wark¹¹*Department of Physics, Clarendon Laboratory, University of Oxford, Parks Road, Oxford OX1 3PU, United Kingdom*²*Lawrence Livermore National Laboratory, Livermore, California 94551, USA*³*CONICET and Instituto de Ciencias Básicas, Universidad Nacional de Cuyo, Mendoza 5500, Argentina*⁴*AWE, Aldermaston, Reading, RG7 4PR, United Kingdom*

(Received 5 October 2011; published 13 January 2012)

The compression of solids by a ramped pressure pulse, as opposed to shock compression, affords the potential to create states of solid-state matter at pressures greater than those achievable in diamond anvil cells. A fundamental understanding of this process requires a knowledge of the loading conditions that discriminate between so-called quasi-isentropic (QI) conditions and those pertaining to the higher entropy states produced by shock loading. We present here molecular dynamics simulations of single-crystal copper deformed over a range of strain rates and demonstrate that QI states at high pressure and low temperature can be present even at strain rates in excess of 10^{12} s^{-1} . These states survive long enough to be studied with novel ultrafast techniques, in principle allowing simple, compact, isentropic compression experiments. Our atomistic simulations, with up to 25 million atoms, simulated for ramp durations of up to 300 ps, show how plastic deformation and melting varies with strain rate.

DOI: [10.1103/PhysRevB.85.024112](https://doi.org/10.1103/PhysRevB.85.024112)

PACS number(s): 07.35.+k

I. INTRODUCTION

Over the past few years there has been a growing interest in so-called isentropic compression experiments (ICEs), which rely on loading a material to high pressure via ramp, rather than shock, compression.¹⁻⁴ At the outset it is important to note that the name itself is somewhat of a misnomer, as even in a slow ramp compression plastic work will result in the production of heat, and perhaps the nomenclature quasi-isentropic (QI) is more apt.

One of the main motivations for such QI compression experiments is to produce novel states of solid-state matter that cannot be accessed by other high-pressure techniques. Much of our knowledge of the physical properties of solid matter under high compression has been obtained by compressing materials statically within diamond anvil cells (DACs).⁵ While progress is being made in this field toward higher pressures, the technique may ultimately be constrained by the limiting strength of the diamonds themselves, and at the present time experiments above pressures of order 350 GPa appear difficult.

Much higher pressures can be generated by the shock compression of matter, and there exists a variety of different loading mechanisms, such as gas guns, explosives, flyer plates, magnetic loading, and laser ablation, to name but a few.⁶ Indeed, it is the latter technique that has produced some of the highest pressures achievable in the laboratory, with close to a Gbar (100 TPa) having been reported.⁷ However, single-shock compression is not a technique that can be applied if one wishes to keep a material solid at high pressure: The shock compression process by its very nature produces a highly entropic state behind the shock front, along with an associated rise in temperature, and this temperature rise increases more quickly with compression than the melting point.⁸ As a result, most metals undergo melting when shocked to pressures between approximately 100 and 300 GPa.

On the other hand, if the pressure pulse is applied on a time scale that is long compared with the shock rise time (but still far shorter than any static technique) then it is possible to achieve high pressures by dynamic loading. Indeed,

initial experiments using laser ablation as the driver have demonstrated that diamond can be ramp compressed over several nanoseconds to 800 GPa, with evidence of strength demonstrating that it remained in the solid phase.⁴ The growth of interest in such high-pressure states of solid-state matter is related to the possibility of studying areas of the phase diagram of materials that have hitherto proved elusive. For example the thermodynamic properties of such high-pressure solid-state matter in the TPa regime is of relevance to a large number of questions in high-energy-density physics, as well as being of relevance to the study of the cores of the giant planets.⁹ It is in this context that we present here molecular dynamics simulations of ramp-compressed single-crystal copper. Our aim is to start to investigate the sort of time scales that separate shock compression from QI compression, and to confirm that molecular dynamics (MD) predicts that it is indeed possible to keep a material close to an isentrope even at extremely high strain rates.

The paper is laid out in the following manner. We first present molecular dynamics simulations of the simple case of elastic compression of a solid. In this case we demonstrate the expected result that the material remains close to an isentrope if the time scale for compression is long compared with the fastest phonon period within the system. We then consider three-dimensional materials that exhibit plastic flow at high pressures. We argue that the material will be QI compressed if the rise time of the ramp is long compared with the expected shock rise time for that particular peak pressure—a figure that can be deduced from the Swegle-Grady relation.^{10,11} When applied to copper, we deduce that QI compression of copper to ~ 100 to 250 GPa should be possible with ramp rise times corresponding to strain rates slow compared with 10^{13} s^{-1} . We use molecular dynamics simulations at strain rates between 10^9 and just above 10^{12} s^{-1} to verify these predictions. Owing to the nonlinear compressibility of the material, the ramp wave will steepen into a shock as it propagates, resulting in only a certain thickness of the target being QI compressed before shock formation, and shock melting at sufficiently high peak

pressures. We study the time for the steepening of the ramp into a shock and compare the results with those deduced from a recent analytic model.¹² We find that, at least for the cases studied here, ramp compression to several hundred GPa is indeed feasible on picosecond time scales at these high strain rates.

II. SIMULATIONS

The molecular dynamics simulations presented here were performed with the LAMMPS code,¹³ using the Cu embedded atom model (EAM) potential developed by Mishin and co-workers.¹⁴ This potential has previously been fitted to high-pressure data and has been shown to agree well with the experimental shock Hugoniot for Cu.¹⁵

A. Elastic compression simulations

Before studying a complex system, it is instructive to consider a simple elastic response. In a material with a potential such that the sound speed increases with compression, an elastic shock is formed under rapid compression, and in this purely elastic wave the shock front is approximately one atomic spacing thick. Under shock conditions, as the front progresses each atom moves toward its neighbor, reaching the distance of closest approach on a time scale comparable to, or shorter than, a vibrational period. As a result, at a local level, the instantaneous distance between two atoms at the shock front is shorter than the mean spacing in the compressed region behind the front. The high temperature produced by the shock is caused by this “over-compression,” exhibited instantaneously as a large potential energy, which on the time scale of a few vibrational periods is, in part, converted to heat.

In order to demonstrate this, we performed MD simulations of a system of Cu atoms with a 3×3 unit cell cross section. This small cross section inhibits the onset of plasticity and allows investigation of a purely elastic response. We refer to this as a quasi-1D simulation. The system was first thermalized at 10 K, and then a shock was introduced along [001] by fixing the velocity of the first few planes of atoms (usually referred to as the “piston”) raising them from 0 to 700 ms^{-1} in 100 fs. We show in Fig. 1 a plot of the interatomic spacing between two particular atoms, situated thirty lattice spacings from the driven surface, as a function of time. Several things are apparent from the plot. First, before the shock has reached this pair of atoms, the typical vibrational period can be seen to be of order 200 fs, as would be expected for the Debye frequency of Cu modeled with the Mishin potential. The sudden decrease in interatomic spacing takes place on a time scale shorter than this period within the uncompressed material leading to a brief, local overcompression. Subsequently, the vibrational amplitude is seen to substantially increase. This increase in amplitude is associated with the 50 K temperature rise produced during the shock compression.

As the shock width in this quasi-1D elastic case is at the lattice level, and the rise time of the shock of order a phonon period, we would expect that close to isentropic compression could be achieved even with relatively short ramp times. As an example we subject the quasi-1D chain of Cu atoms to the same particle velocity (0.7 km s^{-1}), but now achieve this

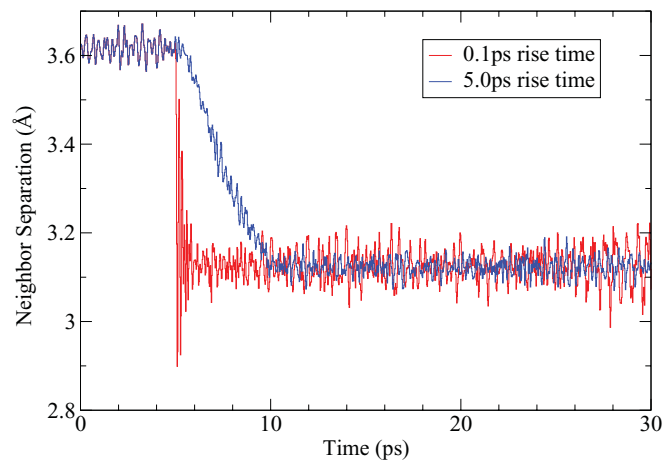


FIG. 1. (Color online) The interatomic spacing as a function of time for two particular atoms in a quasi-1D chain that has been subjected to ramp compressions with rise times of 0.1 ps and 5 ps. Note that the thermal motion is identical in the two cases prior to compression.

by increasing the velocity of the piston linearly over 5 ps (corresponding to a strain rate in excess of $2 \times 10^{10} \text{ s}^{-1}$). The results of this ramp compression are also shown in Fig. 1.

We note that the rms displacement of the atomic motion is considerably smaller in the compressed region when the pressure is applied as a ramp, rather than under shock conditions: The reduction of the interatomic spacing on a time scale long compared with the phonon period has led to close to isentropic conditions. The temperature of the compressed material has been raised by 8 K, even though it can be seen that the rms displacement of the compressed material is less than that of the uncompressed material. Indeed, it has previously been shown that within the Grüneisen formalism, for materials with a Grüneisen parameter exceeding 0.67, under isentropic compression the rms amplitude of the atoms will not only decrease in absolute terms, but also as a fraction of the interatomic spacing.¹⁶ Such a decrease in rms displacement is still consistent with a temperature rise, owing to the change in shape of the potential well within which the atoms are confined.

In Fig. 2 we plot the temperature rise in a series of quasi-1D simulations which were initially thermalized to 300 K. Ramp times between 0.01 and 60 ps, corresponding to strain-rates of approximately 2×10^9 to $2 \times 10^{13} \text{ s}^{-1}$ are shown. It is clear that the temperature rise falls from the shock value to the quasi-isentropic value over a range of ramp times covering the typical phonon periods of a solid—hundreds of fs to several ps. For strain rates below approximately 10^{11} s^{-1} the temperature rise of order 80 K is consistent with isentropic compression (i.e., with a reduction of the lattice parameter from 3.6 to 3.13 Å, an initial temperature of 300 K, and a Grüneisen parameter of 1.7).¹⁶ This trend not only demonstrates the idea that the phonon period sets the time scale for elastic ramp compression of a solid, but hints at a more fundamental idea: The time scale required to compress a solid quasi-isentropically is related to the time scale of the fundamental response of the material. Although this is the phonon lifetime in the case of elasticity, the time scale for plastic deformation would ultimately be set by the rate at which dislocations, or other defects, relieve shear

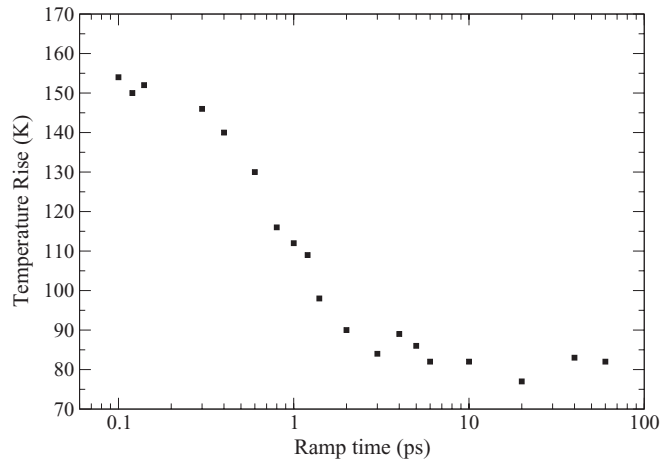


FIG. 2. The temperature rise in a ramped, quasi-1D compression to a maximum piston velocity, $U_p = 0.7 \text{ km s}^{-1}$.

stress.¹⁷ We now investigate this postulate in the context of a full elastoplastic response in Cu.

B. 3D simulations

The situation in a more physically realistic 3D system is considerably more complex than that outlined for the quasi-1D case discussed above. This extra complexity is due to the fact that plastic work and plastic flow can occur, and the width of the shock front is now generally greater than the lattice constant. From the experimental standpoint, it is known that the rise time of a steady shock decreases rapidly with the peak applied stress: This is the well-known Swegle-Grady (SG) relation, $\dot{\epsilon} = A\sigma^n$, where $\dot{\epsilon}$ is the strain, σ the stress, and A a constant that is material dependent.^{10,11} Experimental data demonstrating the SG relation is shown in Fig. 3 (taken from Swegle *et al.*¹¹), showing that this empirical relation appears to hold over a vast range of different materials, with $n \sim 4$. Despite its wide-ranging applicability, our understanding of the origin of the SG relation is still far from complete.¹⁸ However, studies that have been undertaken with MD simulations seem to indicate that a similar relation exists within them as well, though the few studies that have been undertaken to date indicate a slightly lower value of n , closer to 3.3.¹⁹ In any event there appears some merit in using this relation to estimate the strain rates, and hence shock thicknesses, that we might expect for shock compression of Cu to 100–250 GPa.

Extrapolation of the experimental data shown in Fig. 3 to 100 GPa would indicate that the strain rate at this peak pressure is close to 10^{12} s^{-1} , and at 250 GPa would be in excess of 10^{13} s^{-1} . We note that the ultimate strain rate possible (where the shock front is only a lattice spacing thick) typically corresponds to a strain rate of several times 10^{13} s^{-1} . Thus the SG relation predicts that the time scale for shock compression at pressures of order 250 GPa is less than a picosecond—that is to say, even an extremely rapidly rising ramp may result in close to isentropic compression. We note that the extrapolation of the data in Fig. 3 also gives reasonable agreement with the strain rates found in previous molecular dynamics simulations of Cu shock compressed to 35 GPa,

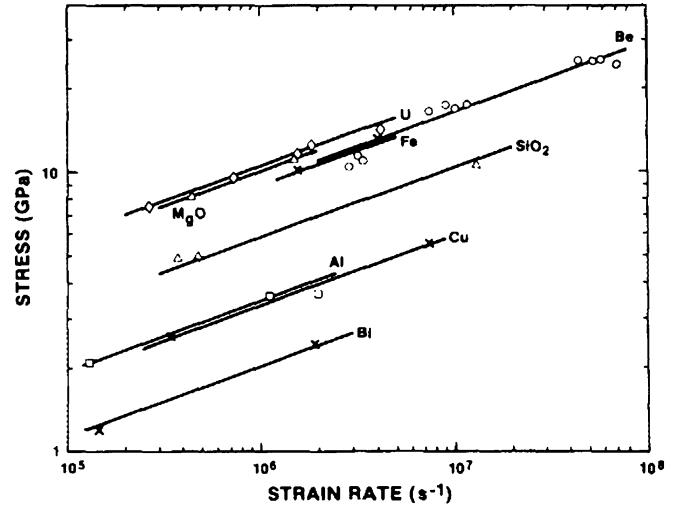


FIG. 3. Experimental data showing the relationship between peak stress in a shock and the strain rate at the shock front: the so-called Swegle-Grady relation. Data taken from Swegle *et al.* [11]. Reprinted with permission from: J. Appl. Phys. 58, 692 (1985). Copyright 1985, American Institute of Physics.

where the time scale for stress relaxation at the shock front was found to be several tens of picoseconds,²⁰ and as we will show later, this strain rate of 10^{13} s^{-1} at around 250 GPa is consistent with the present simulations. Thus, for peak stresses in the 100–250 GPa regime, from a simple application of the SG relation it appears feasible that we should be able to keep Cu close to an isentrope at very high strain rates indeed. For the work presented here, we study Cu ramp compressed at rates of between 10^9 s^{-1} to just above 10^{12} s^{-1} .

We have simulated the ramp compression of copper single crystals with a peak particle velocity applied to the sample of 3.5 km s^{-1} , which corresponds to a peak pressure, in the shock case, of 250 GPa. This value was chosen as it lies above the shock-melt pressure for the Mishin potential, which previous studies have shown lies between 200 and 220 GPa.¹⁵ As in previous studies, the sample was compressed by moving a “piston” of atoms into the sample along the [001] direction at the particle velocity.^{15,20} This velocity was linearly ramped from 0 to the peak particle velocity in rise times ranging from 1 to 300 ps, after which it was held constant. The rise time of these ramps compare well with those used in recent shockless laser compression experiments.^{3,4,21}

The longer the duration of the ramp pulse applied to the sample, the larger will be the sample size required in the simulations. For the longest ramps, of 300 ps duration, the size of the simulated sample was $25 \times 25 \times 10000$ conventional unit cells (25 million atoms), $4 \mu\text{m}$ long along the compression direction, with periodic boundary conditions applied across the (25×25) width of the sample. In all of the simulations the initial temperature of the crystal was 10 K, and was equilibrated before ramp compression. For ramps with shorter rise times, the length of the sample could be reduced: The smallest simulations contained 2 million atoms, but in all cases the number of unit cells perpendicular to the compression direction was at least 25×25 . For the longest ramp, the equivalent strain rate for the material in contact with the piston is just above 10^9 s^{-1} .

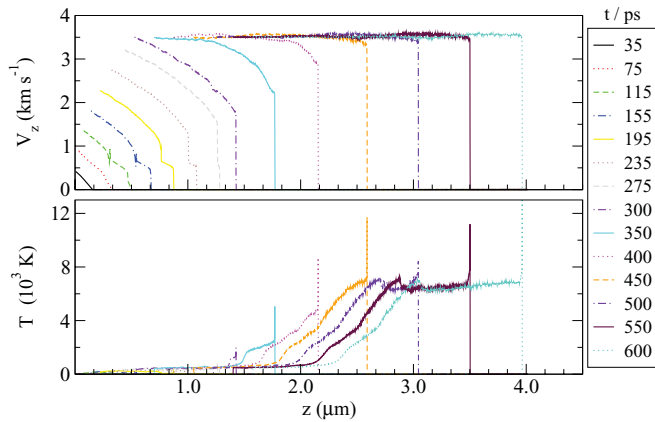


FIG. 4. (Color online) Velocity and temperature profiles for different times during ramp loading of the $0.01 \times 0.01 \times 4 \mu\text{m}$ sample. The linear ramp compression had a rise time of 300 ps and a peak particle velocity of 3.5 km s^{-1} .

In Fig. 4 we show the particle velocity and temperature as a function of depth within the sample for the sample compressed with a linear ramp of 30 ps duration. Profiles are shown for fourteen different times after the start of the ramp, ranging from 35 to 580 ps, at which point the compression wave is close to the end of the $4 \mu\text{m}$ (original length) sample. Several interesting features can be seen in Fig. 4. We note that even though we are applying ramp compression, the gradient in particle velocity quickly starts to steepen, and by 500 ps after the start of the ramp the compression front has steepened sufficiently to become a full shock. Indeed, this is one of the major features of the ICE technique: The ramp wave will have a tendency to steepen, and thus ramp compression can only be achieved for a finite thickness within the sample—a point to which we will return later. It is also clear that for these linear ramps, the steepening process occurs first at the compression front, and a shock is formed here early in the process, although early in the pulse the material is not shocked to the full peak pressure. In principle, it has been shown that if the material response is known in advance, it may be possible to tailor the temporal profile of the ramp compression such that, although steepening of the profile occurs, formation of a shock is delayed for as long as possible—that is to say, ramp compression occurs throughout the pulse, getting steeper and steeper, until finally a shock is formed taking the material to the full peak particle velocity.¹² However, even though we observe some steepening within the sample early in the application of pressure, we see from the temperature profiles that the material closer to the piston is indeed experiencing ramped compression right until the end of the simulation, with the first $1.5 \mu\text{m}$ of the sample, nearest to the piston, only being heated to approximately 500 K, well below the melt temperature of Cu at these compressions (6000 K). In contrast, the last micron or so of material, farthest from the piston, reaches a temperature of 7000 K and, as we will demonstrate below, is molten.

As our initial temperatures are low (10 K), the temperature rise due to compression alone for an isentrope is expected to be negligible, and the heating of the material to 500 K close to the piston is dominated by the plastic work involved in relieving the shear stress induced by the uniaxial compression.

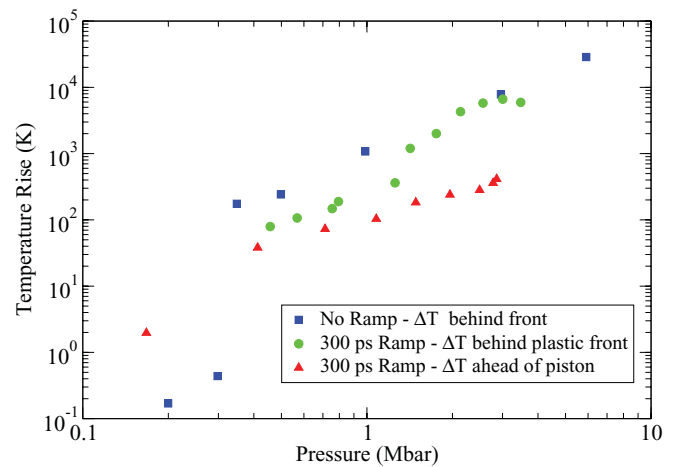


FIG. 5. (Color online) A comparison between temperatures produced by the 300 ps ramp and shock compression. The red triangles show the temperatures and pressures 1 nm from the piston for the ramp. The green circles show the same properties 1 nm behind the foot of the ramp compression pulse. The blue squares show the temperature and pressure 1 nm behind the shock front of a series of separate simulations, within each of which the crystal has been shock compressed to the appropriate pressure.

By the end of the simulation a shock has been formed. An analysis of the strain-rate of the front at this point shows it to be $3 \times 10^{12} \text{ s}^{-1}$, in reasonable agreement with our estimates based on the SG relation.

At very early times, up until 250 ps after the start of compression, the observed sharp rise to a particle velocity of order 0.6 km s^{-1} is the elastic precursor wave: For a perfect Cu crystal modeled by the Mishin potential, the elastic limit is 30 GPa. This elastically compressed region, of about $0.15 \mu\text{m}$ thickness at 150 ps, does not result in a very large temperature rise, as can be seen from Fig. 4, as no plastic work is done in this region.

A further comparison between the conditions produced by this 300 ps ramp and those that would be produced by shock compression can be made by referring to Fig. 5. This figure shows results from both the 300 ps ramp simulation and from a whole series of separate shock simulations. Each of the blue squares shows the temperature and pressure conditions behind the shock front in a given shock simulation, and thus the locus of these data points is effectively plotting the Hugoniot in the P - T plane. Shock-induced melting was found to have occurred at a pressure of 220 GPa and temperature of 6000 K. It can be seen that below 30 GPa there is very little temperature rise in the shock case, and once more this is because only an elastic wave is found in this regime. The red triangles and green circles show the locus of states for the ramp compression just in front of the piston and just behind the foot of the compression front, respectively. From this figure we can see once more that the temperature of the material close to the piston remains significantly cooler for a given pressure than the corresponding conditions within a shock, with a maximum temperature of order 500 K, dominated by plastic work. However, owing to the steepening of the profile into a shock at the foot of the compression pulse, the conditions at this point in the ramped profile quickly approach those of the equivalent shock. As

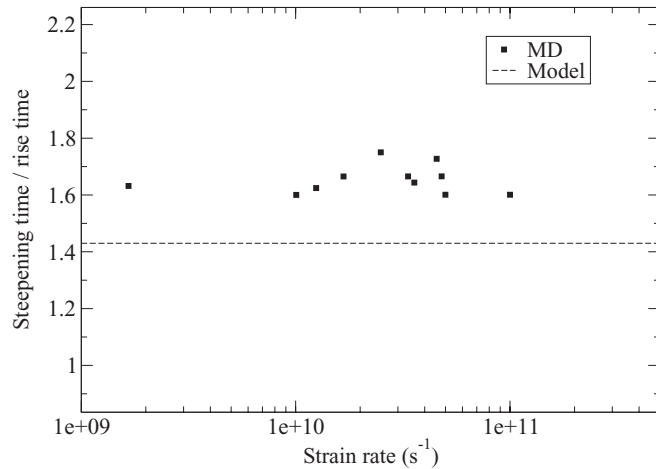


FIG. 6. The ratio of the time taken to steepen into a shock divided by the ramp compression time for simulations at a variety of strain rates for the material just in front of the piston.

noted above, this results in only a finite thickness of the material being kept at the relatively low temperature of 500 K.

It is thus clear that due to profile steepening the ramp compression technique will only allow a certain thickness of material to be compressed in a QI manner before shock formation. For example, from Fig. 4 it is evident that by around 500 ps after the start of the ramp, the material at the front is being shock compressed. We have therefore performed a number of simulations for different ramp rise times, and thus strain rates for the material close to the piston, and studied the time taken for the ramp to steepen such that the particle velocity at the front of the ramp is the peak particle velocity of 3.5 km s^{-1} . The results are shown in Fig. 6 for strain rates between just over 10^9 s^{-1} and just above 10^{12} s^{-1} . As found by Swift and co-workers¹² over a wide range of strain rates the time taken for steepening is of order 1.5 times the rise time of the ramp. Once the ramp strain rate exceeds $5 \times 10^{11} \text{ s}^{-1}$, assigning a time for steepening becomes difficult. This is both because we are now starting to approach the same strain rate we would expect for the steady shock at this pressure (and hence little steepening is required), and also because both the ramp and shock thickness are only a couple of lattice spacings, and thus attempting to diagnose the difference between the ramp and the shock becomes somewhat arbitrary. Alongside the MD results, we also show the predictions for this ratio based on a very simple model. In this model we assume a linear Hugoniot, $U_s = C_0 + s_1 U_p$, where U_s is the shock velocity, C_0 the speed of sound, U_p the particle velocity, and s_1 a constant. We assume that the foot of the ramp moves at C_0 , while the top of the ramp moves at the instantaneous velocity given by the above equation. Steepening occurs when the top of the ramp catches up with the bottom. Within this model the time for steepening is then given by $t_{\text{rise}}[C_0 + (s_1 - 0.5)U_p]/(s_1 U_p)$. For our simulations, where $C_0 = 4 \text{ km s}^{-1}$, $s_1 = 1.5$, and $U_p = 3.5 \text{ km s}^{-1}$, we find that the ratio of the steepening time to the rise time is 1.43.

Evidently once the material has steepened into a shock, the temperature rises are large. An analysis of the centrosymmetry parameter (CSP) in these high-temperature regions implies that the material close to the piston is molten in these cases. In

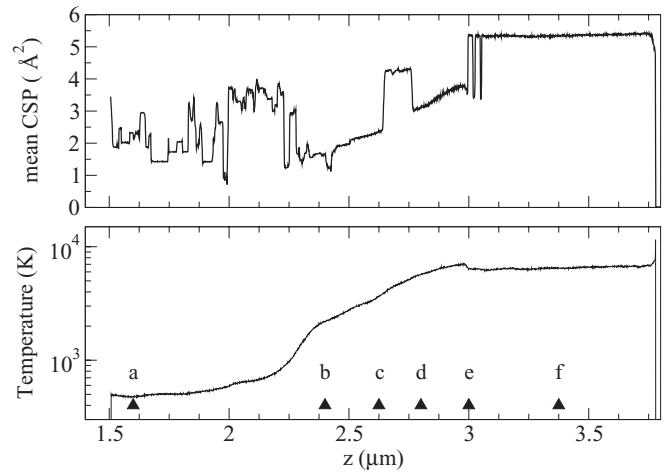


FIG. 7. The CSP and temperature as a function of distance for the 300 ps ramp taken 580 ps after the start of the ramp. The triangular markers indicate the center of the 6 regions for which we have calculated the pair correlation function shown in Fig. 8.

Fig. 7 we show the CSP and the temperature as a function of distance within the sample that has been ramp compressed over a 300 ps duration, with the output taken 580 ps after the start of the ramp. However, on its own the CSP is not necessarily a fool-proof indicator of melt (the change in CSP could also be an indication of a defective or amorphous, rather than molten, state). We have thus confirmed the onset of melting with three further diagnostics: the pair correlation function $g(r)$, simulated x-ray diffraction, and a measurement of the diffusivity. Six regions labeled (a)–(f) are shown in Fig. 7, ranging from a position close to the piston (where the material is solid) to one close to the end of the sample (where we demonstrate that the material is molten). For each of these regions we take the atoms in a slice of the simulation 9 nm thick along the ramp compression direction, and plot the pair correlation function $g(r)$ for each region, as shown in Fig. 8. It can be seen that region (a), close to the piston, has very well defined peaks, as this region corresponds to the cold QI compressed material. Regions (b) and (c) have slightly broader peaks in $g(r)$, with lower peak intensities, owing to

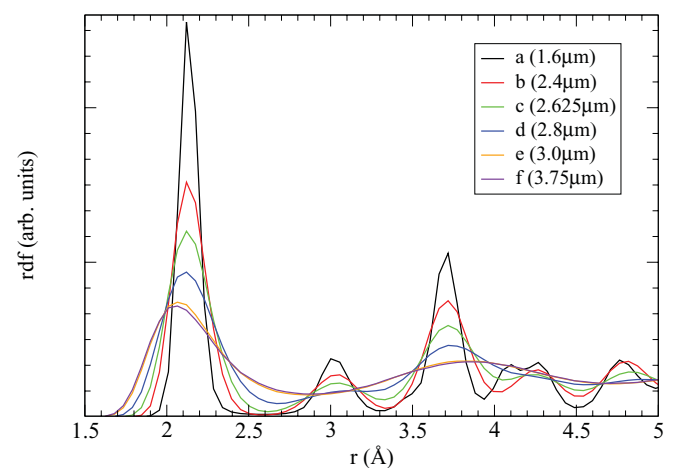


FIG. 8. (Color online) The pair correlation function for positions (a) to (f) shown in Fig. 7.

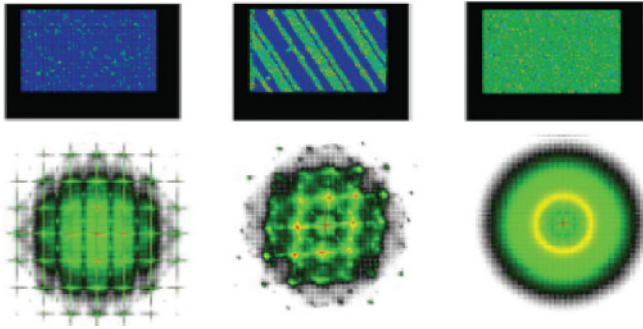


FIG. 9. (Color online) Simulated x-ray diffraction for a perfect Cu crystal, a plastically strained but solid phase—region (b) in Fig. 7—and the molten region close to the shock front—region (e) in Fig. 7. The slice in reciprocal space is perpendicular to the compression direction.

temperature effects. The peak structure for regions (e) and (f) however is consistent with melting, with (d) appearing to be mixed phase.

However, real-space order parameters such as CSP can be difficult to interpret in high-temperature systems. We therefore provide evidence for melting at the shock front from the more reliable method of simulated x-ray diffraction—that is to say, looking at the sample in reciprocal space.²² It should be noted that far from being an just another analysis method, experimental analogs in the form of *in situ*, picosecond x-ray diffraction techniques allow even dynamically compressed materials to be interrogated on relevant time scale.^{23–27}

In Fig. 9 we show slices of reciprocal space which are perpendicular to the compression direction for (a) a perfect uncompressed crystal, (b) a region that has been ramp compressed, but remains solid, and (c) the region that has melted close to the shock front. Distinct Bragg spots can be seen in the solid phase, whereas in the liquid region close to the shock front, diffraction rings, corresponding to a liquid, are clearly evident.

Conclusive verification of melting close to the shock front has also been undertaken by measuring the diffusivity of the system (which is negligible for a solid in MD simulations), and comparing it with the diffusivity of known molten samples. By tracking the motion of individual atoms in the system we have measured the diffusivity of the atoms in the molten region of a 250 GPa shock compressed sample and in the ramp compressed sample in region (f) shown in Fig. 7. In both cases we find the diffusivity to be $\sim 6 \times 10^{-9} \text{ m}^2 \text{ s}^{-1}$. This value is consistent with that found experimentally for molten copper²⁸ and is also in good agreement with that found in previous MD simulations that have studied the solid to liquid transition.²⁹

III. DISCUSSION

The MD simulations presented here indicate that the technique of QI compression, resulting in keeping a material solid at very high pressures, can be achieved even for extremely high strain rates. In the particular case studied, that of single-crystal Cu compressed along the [001] direction to a peak pressure of 250 GPa, the SG relation predicts that the strain rate present within a shock would be several times 10^{12} s^{-1} ,

close to the ultimate limit of that corresponding to a shock thickness of order a lattice spacing. The simulations appear to confirm the assumption that QI conditions can be achieved by ramp compression if the strain rate is kept at several times that of the equivalent shock. That said, the ramp quickly steepens into a shock. We have found that this steepening time is a factor of approximately 1.6 times the ramp rise time over a large range of strain rates (10^9 to 10^{12} s^{-1}). This finding is in good agreement with previous hydrodynamic simulations and an analytic model.¹²

As a result of this ramp steepening, only a thin layer of the crystal can be kept in the solid phase. For the longest ramp studied—that of 300 ps duration—this thickness is of order $1.5 \mu\text{m}$. As we have seen from our simulations, a good diagnostic of the phase and density of the material can be obtained by observing the reciprocal lattice—that is to say, by use of x-ray diffraction. Indeed, over the past few years x-ray diffraction on a picosecond time scale has become an established experimental technique for probing the conditions within shock-compressed samples,^{23,30–32} and successful subnanosecond diffraction from $2 \mu\text{m}$ thick Cu crystals has already been demonstrated.³² We thus conclude that QI compression experiments on the subnanosecond time scale, with strain rates well in excess of 10^9 s^{-1} , are feasible. Indeed, experiments with ramp compression time scales of order 10 ns and strain rates in the region of 10^8 s^{-1} have already been performed on aluminum (which, as can be seen from Fig. 3, should have similar shock rise times to Cu). Ramp compression to 200 GPa has been achieved at these strain rates, and in this work the authors argue, as do we, that QI compression should occur if the strain rate is long compared with the equivalent shock strain rate for the same peak pressure.²

However, it should be borne in mind that if we assume that the strain rates that separate QI compression from shock compression are linked to the shock thickness, and the latter quantity can be determined from the SG relation, then the precise strain rates required for QI compression will be determined by the material-dependent constant A in the SG formula. As can be seen from Fig. 3, for many materials this constant is considerably larger than found in Cu, and as a result the strain rate within a shock for a given shock pressure will be considerably lower than in Cu. For these materials, longer time scales may be required to ensure QI compression, and a study of such materials is certainly worthy of future investigation. On the other hand, we also note that the higher the peak pressure, the smaller the steady-shock thickness, and such scaling bodes well for achieving ultrahigh QI compression on short time scales.

The route to more sophisticated molecular dynamics simulations of QI compression is clear. First, it would be of interest to study nonlinear compression profiles where the time dependence of the compression is better tailored to keeping the profile from steepening into a shock until the last possible moment (as has been studied analytically by Swift *et al.*¹²). Second, here we have studied the response of a perfect single crystal of copper. There is clear interest in looking at both single crystals containing initial defects that could act as sources of dislocations, as well as looking at polycrystalline material. Finally we note that given that the main aim of QI

techniques is to reach hitherto unattainable pressure regimes, there is a pressing need to further develop potentials for classical MD simulations that will retain their validity at these extreme conditions. Many of these further developments will require larger and more complex simulations than those that we have presented here in order to model these as-yet unexplored regions of the phase diagram of solid-state matter.

ACKNOWLEDGMENTS

The authors would like to thank P. Erhart, M. Meyers, J. McNaney, and J. Colvin for fruitful discussions and useful comments. The work at LLNL was performed under the auspices of the US Department of Energy and Lawrence Livermore National Laboratory. A.H. is grateful for support from AWE.

-
- ¹J.-P. Davis, *J. Appl. Phys.* **99**, 103512 (2006).
²K. Lorenz, M. Edwards, A. Jankowski, S. Pollaine, R. Smith, and B. Remington, *High Energy Density Physics* **2**, 113 (2006).
³R. Smith, S. Pollaine, S. Moon, K. Lorenz, P. Celliers, J. Eggert, H.-S. Park, and G. Collins, *Phys. Plasmas* **14**, 057105 (2007).
⁴D. K. Bradley, J. H. Eggert, R. F. Smith, S. T. Prsbrey, D. G. Hicks, D. G. Braun, J. Biener, A. V. Hamza, R. E. Rudd, and G. W. Collins, *Phys. Rev. Lett.* **102**, 075503 (2009).
⁵A. Jayaraman, *Rev. Mod. Phys.* **55**, 65 (1983).
⁶M. Meyers, *Dynamic Behavior of Materials* (John Wiley and Sons, 1994).
⁷R. Cauble, D. W. Phillion, T. J. Hoover, N. C. Holmes, J. D. Kilkenney, and R. W. Lee, *Phys. Rev. Lett.* **70**, 2102 (1993).
⁸Y. B. Zel'dovich and Y. P. Raizer, *Physics of Shock Waves and High-Temperature Hydrodynamic Effects* (Dover, New York, 1966-1967).
⁹M. Itoh, M. Katayama, and R. Rainsberger, *Mater. Sci. Forum* **465-466**, 73 (2004).
¹⁰D. E. Grady, *Appl. Phys. Lett.* **38**, 825 (1981).
¹¹J. W. Swegle and D. E. Grady, *J. Appl. Phys.* **58**, 692 (1985).
¹²D. C. Swift, R. G. Kraus, E. N. Loomis, D. G. Hicks, J. M. McNaney, and R. P. Johnson, *Phys. Rev. E* **78**, 066115 (2008).
¹³S. Plimpton, *J. Comput. Phys.* **117**, 1 (1995).
¹⁴Y. Mishin, M. J. Mehl, D. A. Papaconstantopoulos, A. F. Voter, and J. D. Kress, *Phys. Rev. B* **63**, 224106 (2001).
¹⁵E. M. Bringa, J. Cazamias, P. Erhart, J. Stölken, N. Tanushev, B. Wirth, R. Rudd, and M. Caturla, *J. Appl. Phys.* **96**, 3793 (2004).
¹⁶W. J. Murphy, A. Higginbotham, J. S. Wark, and N. Park, *Phys. Rev. B* **78**, 014109 (2008).
¹⁷A. Higginbotham, E. M. Bringa, J. Marian, N. Park, M. Suggit, and J. S. Wark, *J. Appl. Phys.* **109**, 063530 (2011).
¹⁸D. E. Grady, *J. Appl. Phys.* **107**, 013506 (2010).
¹⁹B. L. Holian and P. S. Lomdahl, *Science* **280**, 2085 (1998).
²⁰E. M. Bringa, K. Rosolankova, R. E. Rudd, B. A. Remington, J. S. Wark, M. Duchaineau, D. H. Kalantar, J. Hawreliak, and J. F. Belak, *Nature Mater.* **5**, 805 (2006).
²¹J. Edwards *et al.*, *Phys. Rev. Lett.* **92**, 075002 (2004).
²²G. Kimminau, P. Erhart, E. M. Bringa, B. Remington, and J. S. Wark, *Phys. Rev. B* **81**, 092102 (2010).
²³D. H. Kalantar *et al.*, *Phys. Rev. Lett.* **95**, 075502 (2005).
²⁴S. J. Turneaure, Y. M. Gupta, K. Zimmerman, K. Perkins, C. S. Yoo, and G. Shen, *J. Appl. Phys.* **105**, 053520 (2009).
²⁵W. J. Murphy *et al.*, *J. Phys. Condens. Matter* **22**, 065404 (2010).
²⁶M. Suggit, G. Kimminau, J. Hawreliak, B. Remington, N. Park, and J. Wark, *Rev. Sci. Instrum.* **81**, 083902 (2010).
²⁷J. A. Hawreliak *et al.*, *Phys. Rev. B* **83**, 144114 (2011).
²⁸J. Henderson and L. Yang, *Trans. Metall. Soc. AIME* **221**, 72 (1961).
²⁹A. Suzuki and Y. Mishin, *J. Mater. Sci.* **40**, 3155 (2005).
³⁰J. S. Wark, R. R. Whitlock, A. A. Hauer, J. E. Swain, and P. J. Solone, *Phys. Rev. B* **40**, 5705 (1989).
³¹P. A. Rigg and Y. M. Gupta, *Phys. Rev. B* **63**, 094112 (2001).
³²A. Loveridge-Smith *et al.*, *Phys. Rev. Lett.* **86**, 2349 (2001).